Optimal transmit beamforming for near-field integrated sensing and wireless power transfer systems

Ping Sun, Haibo Dai, and Baoyun Wang*

Abstract: The integrated sensing and wireless power transfer (ISWPT) technology, in which the radar sensing and wireless power transfer functionalities are implemented using the same hardware platform, has been recently proposed. In this paper, we consider a near-field ISWPT system where one hybrid transmitter deploys extremely large-scale antenna arrays, and multiple energy receivers are located in the near-field region of the transmitter. Under such a new scenario, we study radar sensing and wireless power transfer performance trade-offs by optimizing the transmit beamforming vectors. In particular, we consider the transmit beampattern matching and max-min beampattern gain design metrics. For each radar performance metric, we aim to achieve the best performance of radar sensing, while guaranteeing the requirement of wireless power transfer. The corresponding beamforming design problems are non-convex, and the semi-definite relaxation (SDR) approach is applied to solve them globally optimally. Finally, numerical results verify the effectiveness of our proposed solutions.

Key words: radar sensing; near-field wireless power transfer; integrated sensing and wireless power transfer (ISWPT); beamforming design

1 Introduction

Radar sensing has been identified as one of the key technologies for future 6G networks, to support many new applications such as Internet of Everything (IoE) applications, unmanned aerial vehicle (UAV) networks, and advanced cross-reality (XR) applications[1, 2]. Therefore, radar sensing technology has gained a lot of research interest from both academia[3, 4] and industry[5]. Meanwhile, the radio frequency based wireless power transfer (WPT), enabling the charge of low-power devices (such as IoE devices) over the air, has also been regarded as a key enabling technology for future wireless networks[6, 7]. It is worth noting that although both radar sensing and WPT are promising functionalities, they are studied and implemented using two separate subsystems conventionally.

Inspired by the idea of dual-functional radar communication (DFRC) where both radar and communication functionalities are jointly designed and implemented using the same hardware platform[8, 9], the authors in Ref. [10] proposed a novel concept of integrated sensing and wireless power transfer (ISWPT). In ISWPT systems, a hybrid transmitter is capable of providing the services of radar sensing and WPT simultaneously. As such, ISWPT has many potential advantages in terms of reducing the system's physical size, cost, and power consumption, as well as alleviating the issues of electromagnetic compatibility and spectrum congestion[10]. These evident advantages of ISWPT over conventional individual radar sensing and WPT make it become an exciting and promising area of research.

In the pioneering work[10], the authors optimized the transmit beamforming vectors for characterizing the fundamental trade-off between radar sensing and WPT,

- Ping Sun and Baoyun Wang are with the School of Communication and Information Engineering, Nanjing University of Posts and Telecommunications, Nanjing 210003, China. E-mail: {2018010214, bywang}@njupt. edu.cn.
- Haibo Dai is with the School of Internet of Things, Nanjing University of Posts and Telecommunications, Nanjing 210003, China. E-mail: hbdai@njupt.edu.cn.
- ∗ To whom correspondence should be addressed.
  Manuscript received: 2022-12-18; accepted: 2022-12-23

considering the case of far-field operation. As extremely large-scale antenna arrays are deployed, especially at high-frequencies, wireless devices (such as WPT devices) are likely located in the near-field region of the transmitter[11−14]. Different from the far-field region, where the wavefront is planar, in the near-field, the wavefront is spherical. The near-field spherical wavefront enables the beam focusing capability, which can be leveraged to facilitate near-field multi-user communications[15−17] or wireless power transfer[18−20]. For example, the authors in Ref. [19] studied the near-field WPT with dynamic metasurfaces antennas and illustrated that focused energy beams can not only enhance energy transfer efficiency but also reduce energy pollution.

Motivated by the above observations, in this paper, we consider the near-field ISWPT scenario, where one hybrid transmitter equipped with an extremely large-scale antenna array serves radar sensing and wireless power transfer simultaneously. As the energy receivers need to be deployed close to the transmitter in general, we consider the energy receivers are located in the near-field region of the transfer antenna, whereas the potential radar targets are located in the far-field region of the transmitter. Under such a scenario, we study the beamforming design at the transmitter to balance the performance of radar sensing and wireless power transfer. The main contributions of this paper are summarized as follows.

● To the best of our knowledge, this work is the first that studies the near-field ISWPT systems, considering the energy receivers are located in the near-field region of the base station (BS) with extremely large-scale antenna arrays. The BS charges multiple single-antenna energy receivers and senses several potential target directions simultaneously, and the beamforming vectors of BS are optimized to balance these two functionalities.

● For radar sensing, both the metrics of classical beampattern matching and the emerging max-min beampattern gain are considered. For each radar performance metric, we formulate a dedicated optimization problem to maximize the performance of radar sensing, while guaranteeing the requirements of

wireless power transfer. The formulated beamforming design problems are non-convex, and the semi-definite relaxation (SDR) approach is applied to solve them globally optimally.

● Finally, the numerical results are provided to verify the effectiveness of our proposed design. By considering the near-field effect, our proposed design significantly outperforms the far-field benchmark schemes in terms of beampattern matching accuracy and extra harmful beam-free.

Notation: Scalars, vectors, and matrices are denoted by lower letters, bold-face lower-case letters, and bold-face upper-case letters, respectively (e.g., x, $\boldsymbol{x}$, and $\boldsymbol{X}$, respectively). For a matrix $\boldsymbol{X}$, $\boldsymbol{X} \succeq \boldsymbol{0}$ means that $\boldsymbol{X}$ is positive semidefinite matrix, and $\boldsymbol{X}^{\mathrm{H}}$ denotes its Hermitian operator.

2 System model and problem formulation

2.1 Signal and system models

We consider a near-field ISWPT system as shown in Fig. 1, where one hybrid base station (BS) sends wireless signals to charge K single-antenna energy receivers and to perform radar sensing over a potential area simultaneously. The BS employs an extremely large-scale uniform linear array with N antenna elements. The antenna spacing is $d = \dfrac{\lambda}{2}$, with λ denoting the carrier wavelength. The boundary between the near-field region and the far-field region is referred to as the Rayleigh distance[11, 12], which is defined as
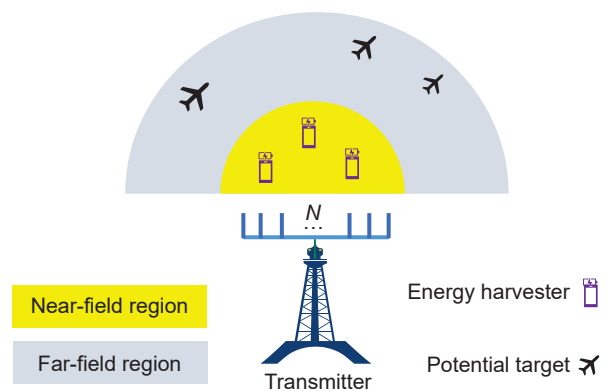
Fig. 1 Illustration of near-field ISWPT scenario, where one extremely large-scale antenna array charges multiple energy receivers (located in the near-field) and senses several potential targets (located in the far-field) simultaneously.

$d_F = \dfrac{2D^2}{\lambda}$, with D denoting the antenna array aperture. In our setting, the antenna array aperture $D = (N-1)d$, and the strong near-field region can be up to tens of meters for a middle-size antenna array. In practice, energy receivers need to be deployed close to the BS because they have poorer sensitivity[21, 22]. Therefore, we consider the energy receivers are located in the near-field region of BS. While for radar sensing, the potential targets are assumed to be located in the far-field region of BS.

Considering the fact that radar signals can be utilized to realize radar sensing and wireless power transfer simultaneously, we assume the BS uses N radar beams for potential target sensing and wireless power transfer. Thus, the baseband transmitted signal of BS, denoted by $x \in \mathbb{C}^{N \times 1}$, is given by

$$x = \sum_{i=1}^{N} w_i s_i \tag{1}$$

where $w_i \in \mathbb{C}^{N \times 1}$ denotes the i-th radar sensing beamforming vector and s_i denotes the i-th radar waveform with zero mean and unit variance. It is assumed that $\{s_i\}$ are independent.

Based on Eq. (1) and considering that the radar waveform s_i has a unit power. The per-antenna transmit power constraint at the BS can be formulated as

$$\left[\sum_{i=1}^{N} w_i w_i^{\mathrm{H}} \right]_{n,n} \leqslant \frac{P_t}{N}, \quad n = 1, 2, \ldots, N \tag{2}$$

where P_t denotes the maximum transmit power budget and $[\cdot]_{n,n}$ denotes the (n,n)-entry of a matrix.

Let $p_n = (0, (n-1)d)$ denotes the Cartesian coordinate of the n-th antenna element of BS. Then, under the free-space condition, the near-field wireless channel between the BS and the k-th energy receiver located in $p_k = (x_k, y_k)$ can be given by[14]

$$[h_k]_n = \sqrt{\left(\frac{c}{4\pi f_c d_n^k} \right)^2} \, \mathrm{e}^{-\mathrm{j}2\pi f_c \frac{d_n^k}{c}} \tag{3}$$

where $h_k \in \mathbb{C}^{N \times 1}$ denotes the near-field wireless channel between the BS and the k-th energy receiver, with $[h_k]_n$ representing the n-th element of h_k; c and f_c denote the light speed and the carrier frequency, respectively; and $d_n^k \triangleq |p_n - p_k|$ denotes the distance between the n-th

antenna element of BS and the k-th energy receiver.

According to Eqs. (1) and (3), the harvested energy of the k-th energy receiver can be written as[21, 22]

$$E_k(\{w_i\}) = \zeta \sum_{i=1}^{N} \left| h_k^{\mathrm{H}} w_i \right|^2, \forall k \in \mathcal{K} \tag{4}$$

where $0 < \zeta < 1$ denotes the energy conversion efficiency at the energy receiver.

For radar sensing, we focus on the transmit beampattern design, which has been widely used in the field of multiple-input multiple-output (MIMO) radar[23]. For our considered ISWPT system, both the energy signal and radar waveform can be used to perform radar sensing. Therefore, the corresponding transmit beampattern gain can be formulated as

$$\mathcal{B}(\theta) = E\left[\left\| a^{\mathrm{H}}(\theta) \left(\sum_{i=1}^{N} w_i s_i \right) \right\|^2 \right] = \\ a^{\mathrm{H}}(\theta) \left(\sum_{i=1}^{N} w_i w_i^{\mathrm{H}} \right) a(\theta) \tag{5}$$

where $a(\theta)$ represents the steering vector at angle θ, given by

$$a(\theta) = \left[1 \quad \mathrm{e}^{\mathrm{j}2\pi \frac{d}{\lambda} \sin\theta} \quad \ldots \quad \mathrm{e}^{\mathrm{j}2\pi \frac{d}{\lambda}(N-1)\sin\theta} \right]^{\mathrm{T}} \tag{6}$$

For radar sensing, one of the widely used design metrics is called the beampattern matching, where the radar beams are designed to match a given desired beampattern[23]. The radar performance can be evaluated by the matching error function, given by

$$L(\{w_i\}, \alpha) = \\ \frac{1}{L} \sum_{l=1}^{L} \left| \alpha \bar{\mathcal{B}}(\theta_l) - a^{\mathrm{H}}(\theta_l) \left(\sum_{i=1}^{N} w_i w_i^{\mathrm{H}} \right) a(\theta_l) \right|^2 \tag{7}$$

where α is a scaling factor; and $\left\{ \bar{\mathcal{B}}(\theta_l) \right\}_{l=1}^{L}$ denotes the given desired beampattern, specifying the desired power distribution at the L angles $\{\theta_l\}_{l=1}^{L}$. Based on the radar sensing specific tasks, the pre-designed beampattern can either be uniformly distributed beampattern (e.g., angles are sampled uniformly), or non-uniformly distributed beampattern (e.g., angles are sampled only towards several potential directions). The former pre-designed beampattern is suitable for the task without knowing the direction of radar targets,

while the latter beampattern is beneficial for the application with knowing the potential directions, e.g., for target tracking.

2.2 Problem formulation

The goal of this paper is to design transmit radar beams for achieving the best radar performance while guaranteeing the energy harvesting constraints of energy receivers. Considering first the matching error function defined in Eq. (7) as the radar metric, our interested beamforming design problem can be formulated as

$$
\min_{\{w_i\},\alpha} \frac{1}{L}\sum_{l=1}^{L}\left|\alpha\bar{\mathcal{B}}(\theta_l)-a^{\mathrm{H}}(\theta_l)\left(\sum_{i=1}^{N}w_iw_i^{\mathrm{H}}\right)a(\theta_l)\right|^2
$$
$$
\text{s.t. } \zeta\sum_{i=1}^{N}\left|h_k^{\mathrm{H}}w_i\right|^2 \geqslant e_k, \tag{8}
$$
$$
\left[\sum_{i=1}^{N}w_iw_i^{\mathrm{H}}\right]_{n,n} \leqslant \frac{P_t}{N}, \forall n
$$

where e_k denotes the target harvested energy value of the k-th energy receiver.

In addition to the beampattern matching, the max-min beampattern gain design criterion is also very commonly adopted for evaluating radar performance in Ref. [24]. The key idea of max-min beampattern gain design criterion is to maximize the minimum beampattern gain of several desirable directions/angles $\Theta \triangleq \{\theta_1, \theta_2, \ldots, \theta_L\}$. Then, considering the max-min beampattern gain as the radar metric, the radar beamforming design problem in Formula (8) can be replaced by

$$
\max_{\{w_i\}} \min_{\forall\theta\in\Theta} \ a^{\mathrm{H}}(\theta)\left(\sum_{i=1}^{N}w_iw_i^{\mathrm{H}}\right)a(\theta)
$$
$$
\text{s.t. } \zeta\sum_{i=1}^{N}\left|h_k^{\mathrm{H}}w_i\right|^2 \geqslant e_k, \tag{9}
$$
$$
\left[\sum_{i=1}^{N}w_iw_i^{\mathrm{H}}\right]_{n,n} \leqslant \frac{P_t}{N}, \forall n
$$

We note that both problems (8) and (9) are non-convex with respect to optimization variables $\{w_i\}$.

3 Proposed solution

In this section, we apply the celebrated semidefinite relaxation (SDR) technique to solve problems (8) and (9) globally optimally. Specifically, the globally

optimal solution to problem (8) is provided in Subsection 3.1, and that to problem (9) is presented in Subsection 3.2.

3.1 Optimal beamforming design to problem (8)

In this subsection, we propose the SDR approach to solve the non-convex problem (8) globally optimally. For this purpose, we define a new set of auxilary variables

$$
W_i = w_iw_i^{\mathrm{H}}, \ i = 1, 2, \ldots, N \tag{10}
$$

where $W_i \geq 0$ and $\mathrm{Rank}(W_i) = 1$.

By substituting Eq. (10) into Formula (8), it follows that

$$
\min_{\{W_i\},\alpha} \frac{1}{L}\sum_{l=1}^{L}\left|\alpha\bar{\mathcal{B}}(\theta_l)-a^{\mathrm{H}}(\theta_l)\left(\sum_{i=1}^{N}W_i\right)a(\theta_l)\right|^2
$$
$$
\text{s.t. } \zeta\sum_{i=1}^{N}\mathrm{Tr}\left(W_ih_kh_k^{\mathrm{H}}\right) \geqslant e_k,
$$
$$
\left[\sum_{i=1}^{N}W_i\right]_{n,n} \leqslant \frac{P_t}{N}, \forall n, \tag{11}
$$
$$
W_i \geq 0, \ \mathrm{Rank}(W_i) = 1, \forall i
$$

Problem (11) is still non-convex due to the non-convex rank-one constraint. To handle this challenge, we adopt the SDR approach by ignoring the non-convex rank-one constraint. Then, the relaxed problem of Formula (11) is given by

$$
\min_{\{W_i\},\alpha} \frac{1}{L}\sum_{l=1}^{L}\left|\alpha\bar{\mathcal{B}}(\theta_l)-a^{\mathrm{H}}(\theta_l)\left(\sum_{i=1}^{N}W_i\right)a(\theta_l)\right|^2
$$
$$
\text{s.t. } \zeta\sum_{i=1}^{N}\mathrm{Tr}\left(W_ih_kh_k^{\mathrm{H}}\right) \geqslant e_k,
$$
$$
\left[\sum_{i=1}^{N}W_i\right]_{n,n} \leqslant \frac{P_t}{N}, \forall n, \tag{12}
$$
$$
W_i \geq 0, \ \forall i
$$

Problem (12) is convex quadratic semidefinite programming (QSDP)[23]. Thus, it can be solved directly and efficiently by using existing convex optimization solvers such as CVX[25].

Denote $\{W_i^*\}$ as the globally optimal solution of problem (12). If the rank of each W_i^* is one, e.g., $\mathrm{Rank}(W_i^*) = 1$, $\{W_i^*\}$ is also the globally optimal solution to problem (11). This implies that the rank relaxation on $\{W_i\}$ in Formula (11) does not cause any loss of optimality. Otherwise, the rank-1 approximation (such

as randomization procedure[26]) should be used to find an approximation to problem (11) from $\{W_i^*\}$, which will cause performance loss to some extent in general. Fortunately, we have the following theorem, which proves the optimality of SDR for problem (11).

Theorem 1 There always exists a rank-one optimal solution to problem (11), denoted by $\{\widetilde{W}_i\}$, such that

$$\text{Rank}\left(\widetilde{W}_i\right) = 1, \; i = 1, 2, \ldots, N \tag{13}$$

Proof. To prove Theorem 1, we define $W = \sum_{i=1}^{N} W_i$. The eigenvalue decomposition of W is given by $W = U\Lambda U^{\text{H}}$, with U and Λ denoting the eigenvector matrix and the eigenvalue matrix, respectively.

Define $\widetilde{W} = U\Lambda^{\frac{1}{2}}U^{\text{H}}$ and $\widetilde{W} = [\widetilde{w}_1, \widetilde{w}_2, \ldots, \widetilde{w}_N]$. It is easy to verify that $W = \widetilde{W}\widetilde{W}^{\text{H}} = \sum_{i=1}^{N} \widetilde{w}_i \widetilde{w}_i^{\text{H}}$, because U is a unitary matrix. Hence, we can construct a set of matrices, i.e.,

$$\widetilde{W}_i = \widetilde{w}_i \widetilde{w}_i^{\text{H}}, \; i = 1, 2, \ldots, N \tag{14}$$

Obviously, $\widetilde{W}_i$ in Eq. (14) is rank-one and positive semi-definite. Meanwhile, it is easy to very that $W = \sum_{i=1}^{N} W_i = \sum_{i=1}^{N} \widetilde{W}_i$, implying $\left\{\widetilde{W}_i\right\}$ is capable of achieving the same function value as the $\{W_i\}$. Also, $\left\{\widetilde{W}_i\right\}$ satisfies all the constraints in Formula (12). As a result, $\left\{\widetilde{W}_i\right\}$ are the globally optimal solution to both problems (11) and (12).

Theorem 1 states the existence of the globally optimal solution to problem (12). From the proof process of Theorem 1, we know that the optimal solution to problem (11) can be constructed according to Eq. (14). Accordingly, the optimal solution to problem (8), denoted by $\{w_i^*\}$, can be directly recovered from $\{\widetilde{W}_i\}$, i.e., $w_i^* = \widetilde{w}_i, \forall i$.

3.2 Optimal beamforming design to problem (9)

In this subsection, we aim to solve the non-convex problem (9) globally optimally. To this end, we first introduce a new auxiliary variable τ and then transform Formula (9) into the equivalent form

$$\max_{\{w_i\}, \tau} \; \tau$$
$$\text{s.t.} \; a^{\text{H}}(\theta) \left(\sum_{i=1}^{N} w_i w_i^{\text{H}}\right) a(\theta) \geqslant \tau, \forall \theta \in \Theta,$$

$$\zeta \sum_{i=1}^{N} \left|h_k^{\text{H}} w_i\right|^2 \geqslant e_k,$$
$$\left[\sum_{i=1}^{N} w_i w_i^{\text{H}}\right]_{n,n} \leqslant \frac{P_t}{N}, \forall n \tag{15}$$

Problem (15) is non-convex with respect to optimization variables $\{w_i\}$. We next apply the SDR technique to solve problem (15) globally optimally.

By defining a new set of auxiliary variables $W_i = w_i w_i^{\text{H}}$, $i = 1, 2, \ldots, N$, Formula (15) can be equivalently rewritten as

$$\max_{\{w_i\}, \tau} \; \tau$$
$$\text{s.t.} \; a^{\text{H}}(\theta) \left(\sum_{i=1}^{N} W_i\right) a(\theta) \geqslant \tau, \forall \theta \in \Theta,$$
$$\zeta \sum_{i=1}^{N} \text{Tr}\left(W_i h_k h_k^{\text{H}}\right) \geqslant e_k, \tag{16}$$
$$\left[\sum_{i=1}^{N} W_i\right]_{n,n} \leqslant \frac{P_t}{N}, \forall n,$$
$$W_i \succeq 0, \; \text{Rank}(W_i) = 1, \forall i$$

Problem (16) is still non-convex due to the non-convex rank-one constraint. By dropping the non-convex rank-one constraint, we obtain the relaxed problem of Formula (16):

$$\max_{\{w_i\}, \tau} \; \tau$$
$$\text{s.t.} \; a^{\text{H}}(\theta) \left(\sum_{i=1}^{N} W_i\right) a(\theta) \geqslant \tau, \forall \theta \in \Theta,$$
$$\zeta \sum_{i=1}^{N} \text{Tr}\left(W_i h_k h_k^{\text{H}}\right) \geqslant e_k, \tag{17}$$
$$\left[\sum_{i=1}^{N} W_i\right]_{n,n} \leqslant \frac{P_t}{N}, \forall n,$$
$$W_i \succeq 0, \forall i$$

Problem (17) is a separable semidefinite program (SDP), which is convex and thus can be solved optimally using the existing convex software tools such as CVX.

We next provide Theorem 2, which shows the optimality of the SDR approach for problem (16).

Theorem 2 Let $\{\hat{W}_i\}$ denote the optimal solution to problem (17). Then, the optimal solution to problem (16) can be constructed as

$$\bar{W}_i = \bar{w}_i \bar{w}_i^{\text{H}}, \; i = 1, 2, \ldots, N \tag{18}$$

where $\bar{w}_i$ denotes the i-th column of $\hat{W} \triangleq \hat{U}\hat{\Lambda}^{\frac{1}{2}}\hat{U}^{\text{H}}$, with

$\hat{U}$ and $\hat{\Lambda}$ denoting the eigenvector matrix and the eigenvalue matrix of $R = \sum_{i=1}^{N} \hat{W}_i$, respectively.

Proof. The proof is similar to that for Theorem 1 and thus is omitted for brevity.

4　Numerical evaluations

In this section, numerical results are provided to demonstrate the performance of our proposed optimal beamforming designs in the near-field ISWPT scenario. In our experiments, we consider a uniform linear array having 32 elements (unless otherwise stated) positioned in the y-axis, the carrier frequency is set to be 2.4 GHz. Without loss of generality, we consider $P_t = 10$ W, $K = 1$, and $\zeta = 0.9$. The energy receiver is placed in the x-axis at the point (3 m, 0 m). The near-field wireless channel is generated following the free-space line-of-sight channel model[18]. The desired beampattern consisting of three main beams, whose direction set is $\Theta = \{-30°, 15°, 60°\}$. We consider a uniform sample in the range of $-90°$ to $90°$ with $0.1°$ interval.

For each radar design metric, we compare the performance of our proposed near-field optimal solution with two benchmark schemes: Radar only and Far-field solution. Radar only denotes the scheme without considering energy transmission, which yields the best radar performance and serves as the performance upper bound of radar sensing. Far-field solution is obtained by replacing the accurate near-field energy transmission channel with a conventional far-field channel model, i.e., ignoring the near-field effect.

We first study the beampattern matching design metric in Figs. 2 and 3. In Fig. 2, we show the transmit beampatterns for our proposed optimal solution (termed as "Near-field"), radar only beamforming scheme (termed as "Radar only"), and the Far-field solution (termed as "Far-field"), under the energy transmission threshold $e_0 = -10$ dBm. From Fig. 2, it is observed that the performance of the proposed optimal solution is close to the upper bound of the radar only solution, whereas the far-field solution generates a beam towards the direction of the energy receiver. This beam may result in false detection, and thus, it is
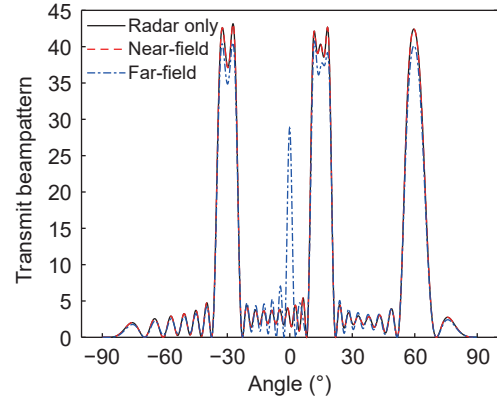
Fig. 2　Transmit beampattern with beampattern matching metric.
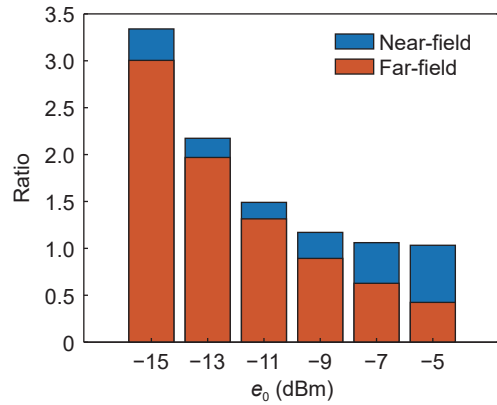
Fig. 3　Energy harvesting ratio versus energy harvesting threshold, under the beampattern matching metric.

harmful to radar sensing. The reason for generating this harmful beam is that the far-field solution uses inaccurate far-field channel modeling to characterize the near-field transmission feature.

In Fig. 3, we plot the energy harvesting ratio over the energy harvesting threshold e_0, where the energy harvesting ratio is defined as the ratio of the practical harvested energy (via the designed beamforming solution) to the energy harvesting threshold e_0. The energy harvesting requirement/constraint is satisfied in practice only when this ratio is greater than one. From Fig. 3, it is observed that our proposed near-field solution can always satisfy the energy harvesting requirement, whereas the far-field solution cannot guarantee this constraint, especially at the high e_0 regime. From Figs. 2 and 3, it is concluded that our proposed near-field optimal beamforming solution outperforms the far-field solution in terms of

beampattern matching, false beam-free, and energy harvesting requirement satisfaction.

Next, we study the max-min design metric in Figs. 4 and 5 . In Fig. 4, we demonstrate the transmit beampatterns of our proposed near-field solution and the two benchmark schemes. Similar to the beampattern matching design, our proposed solution matches the upper-bound beampattern of radar only very well, whereas the far-field solution generates harmful extra beams. This verifies the advantage of our proposed optimal solution taking the near-field effect into account.

Finally, in Fig. 5, we study the effect of the number of antennas at the transmitter on the transmit beampattern. From Fig. 5, it is observed that the performance of our proposed near-field solution is the same as that of the far-field solution when the number of antennas is less than 12. This is caused, in this case, the energy receiver is also located in the far-field
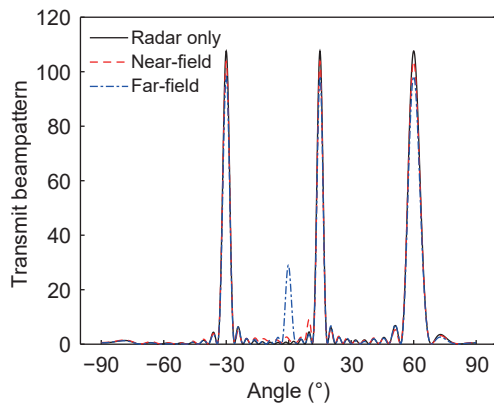
region of the transmitter. However, the performance of our proposed near-field optimal solution is gradually better than the far-field solution as the increase of N. For example, when $N = 32$, the energy receiver is located in the near-field region of the transmitter, and thus the beampattern of our proposed solution is close to the upper-bound achieved by the radar-only solution, which is consistent with the above observations.

5 Conclusion

This paper considered a near-field ISWPT scenario, where the energy receivers are located in the near-field region of the transmitter. Under such a new scenario, we studied the optimal beamforming design problem, considering two radar sensing design criterias: beampattern matching and max-min beampattern gain. For each design criteria, we formulated a beamforming design problem to achieve the best performance of radar sensing, while guaranteeing the requirements of wireless power transfer. Though the formulated problems are non-convex, we solved them globally optimally via applying the technique of SDR. Finally, numerical results demonstrated the effectiveness of our proposed solutions.

Fig. 4   Transmit beampattern with max-min design metric.
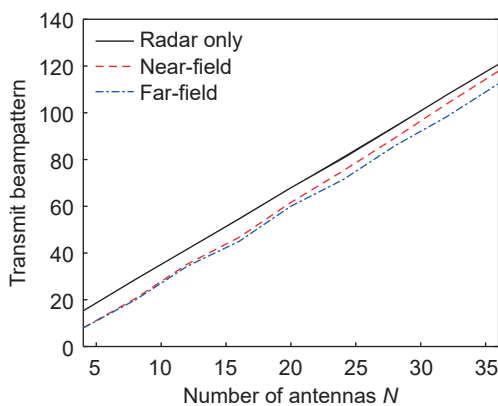
Fig. 5   Transmit beampattern versus the number of antennas N, under the max-min design metric.

Acknowledgment

References

[1]   H. Hong, J. Zhao, T. Hong, and T. Tang, Radar-communication integration for 6G massive IoT services, *IEEE Internet of Things Journal*, vol. 9, no. 16, pp. 14511–14520, 2022.

[2]   A. Bourdoux, A. N. Barreto, B. V. Liempd, C. D. Lima, D. Dardari, D. Belot, E. -S. Lohan, G. Seco-Granados, H. Sarieddeen, H. Wymeersch, et al., 6G white paper on localization and sensing, arXiv preprint arXiv: 2006.01779, 2020.

[3]   A. Behravan, V. Yajnanarayana, M. F. Keskin, H. Chen, D. Shrestha, T. E. Abrudan, T. Svensson, K. Schindhelm, A. Wolfgang, S. Lindberg, et al., Positioning and sensing in 6G: Gaps, challenges, and opportunities, *IEEE Vehicular Technology Magazine*, doi: 10.1109/MVT.2022.

3219999.

[4] C. J. Vaca-Rubio, P. Ramirez-Espinosa, K. Kansanen, Z. -H. Tan, and E. D. Carvalho, Radio sensing with large intelligent surface for 6G, arXiv preprint arXiv: 2111.02783, 2021.

[5] A. Liu, Z. Huang, M. Li, Y. Wan, W. Li, T. X. Han, C. Liu, R. Du, D. K. P. Tan, J. Lu, et al., A survey on fundamental limits of integrated sensing and communication, *IEEE Communications Surveys and Tutorials*, vol. 24, no. 2, pp. 994–1034, 2022.

[6] W. Saad, M. Bennis, and M. Chen, A vision of 6G wireless systems: Applications. trends, technologies, and open research problems, *IEEE Netw.*, vol. 34, no. 3, pp. 134–142, 2020.

[7] B. Clerckx, R. Zhang, R. Schober, D. W. K. Ng, D. I. Kim, and H. V. Poor, Fundamentals of wireless information and power transfer: From RF energy harvester models to signal and system designs, *IEEE J. Sel. Areas Commun.*, vol. 37, no. 1, pp. 4–33, 2019.

[8] T. Huang, N. Shlezinger, X. Xu, Y. Liu, and Y. C. Eldar, MAJoRCom: A dual-function radar communication system using index modulation, *IEEE Trans. Signal Process.*, vol. 68, pp. 3423–3438, 2020.

[9] F. Liu, Y. Cui, C. Masouros, J. Xu, T. X. Han, Y. C. Eldar, and S. Buzzi, Integrated sensing and communications: Toward dual-functional wireless networks for 6G and beyond, *IEEE J. Sel. Areas Commun.*, vol. 40, no. 6, pp. 1728–1767, 2022.

[10] Q. Yang, H. Zhang, and B. Wang, Beamforming design for integrated sensing and wireless power transfer systems, *IEEE Commun. Lett.*, doi: 10.1109/LCOMM.2022. 3216950.

[11] H. Zhang, N. Shlezinger, F. Guidi, D. Dardari, and Y. C. Eldar, 6G wireless communications: From far-field beam steering to near-field beam focusing, arXiv preprint arXiv: 2203.13035, 2022.

[12] M. Cui, Z. Wu, Y. Lu, X. Wei, and L. Dai, Near-field communications for 6G: Fundamentals, challenges, potentials, and future directions, *IEEE Commun. Mag.*, doi: 10.1109/MCOM.004.2200136.

[13] M. Cui and L. Dai, Channel estimation for extremely large-scale MIMO: Far-field or near-field? *IEEE Trans. Commun.*, vol. 70, no. 4, pp. 2663–2677, 2022.

[14] X. Zhang and H. Zhang, Hybrid reconfigurable intelligent surfaces-assisted near-field localization, *IEEE Commun. Lett.*, doi: 10.1109/LCIMM.2022.3215253.

[15] H. Zhang, N. Shlezinger, F. Guidi, D. Dardari, M. F. Imani, and Y. C. Eldar, Beam focusing for near-field multiuser MIMO communications, *IEEE Trans. Wireless Commun.*, vol. 21, no. 9, pp. 7476–7490, 2022.

[16] H. Lu and Y. Zeng, Near-field modeling and performance analysis for multi-user extremely large-scale MIMO communication, *IEEE Commun. Lett.*, vol. 26, no. 2, pp. 277–281, 2022.

[17] H. Lu and Y. Zeng, Communicating with extremely large-scale array/surface: Unified modeling and performance analysis, *IEEE Trans. Wireless Commun.*, vol. 21, no. 6, pp. 4039–4053, 2022.

[18] H. Zhang, N. Shlezinger, F. Guidi, D. Dardari, M. F. Imani, and Y. C. Eldar, Near-field wireless power transfer for 6G internet of everything mobile networks: Opportunities and challenges, *IEEE Commun. Mag.*, vol. 60, no. 3, pp. 12–18, 2022.

[19] H. Zhang, N. Shlezinger, F. Guidi, D. Dardari, M. F. Imani, and Y. C. Eldar, Near-field wireless power transfer with dynamic metasurface antennas, in *Proc. 2022 IEEE 23rd Int. Workshop Signal Process. Advances Wireless Commun.*, Oulu, Finland, 2022, pp. 1–5.

[20] B. J. B. Deutschmann, T. Wilding, E. G. Larsson, and K. Witrisal, Location-based initial access for wireless power transfer with physically large arrays, in *Proc. 2022 IEEE International Conference on Communications Workshops (ICC Workshops)*, Seoul, Republic of Korea, 2022, pp. 127–132.

[21] R. Zhang and C. K. Ho, MIMO broadcasting for simultaneous wireless information and power transfer, *IEEE Trans. Wireless Commun.*, vol. 12, no. 5, pp. 1989–2001, 2013.

[22] L. Liu, R. Zhang, and K. -C. Chua, Secrecy wireless information and power transfer with MISO beamforming, *IEEE Trans. Signal Process.*, vol. 62, no. 7, pp. 1850–1863, 2014.

[23] X. Liu, T. Huang, and Y. Liu, Transmit design for joint MIMO radar and multiuser communications with transmit covariance constraint, *IEEE J. Sel. Areas Commun.*, vol. 40, no. 6, pp. 1932–1940, 2022.

[24] H. Hua, J. Xu, and T. -X. Han, Optimal transmit beamforming for integrated sensing and communication, arXiv preprint arXiv: 2104.11871, 2022.

[25] M. Grant and S. Boyd, CVX: Matlab software for disciplined convex programming, version 2.2, http://cvxr. com/cvx/, 2020.

[26] Z. -Q. Luo, W. -K. Ma, A. M. -C. So, Y. Ye, and S. Zhang, Semidefinite relaxation of quadratic optimization problems, *IEEE Signal Processing Magazine*, vol. 27, no. 3, pp. 20–34, 2010.

Ping Sun received the BS and MS degrees from Nanjing University of Aeronautics and Astronautics, Nanjing, China in 2009 and 2012, respectively. She is currently pursuing the PhD degree in the School of Communication and Information Engineering, Nanjing University of Posts and Telecommunications. Her research interests focus on wireless power transfer, joint radar and communications, and physical-layer security.
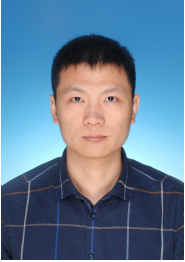
Haibo Dai received the MS degree from Yanshan University, Qinhuangdao, China in 2013, and the PhD degree in electrical engineering from Southeast University, Nanjing, China in 2017. Since February 2018, he has been a faculty member with the School of Internet of Things, Nanjing University of Posts and Telecommunications. His current research interests include wireless resource allocation and management, vehicle-to-everything communications, unmanned aerial vehicle communications, optimization in space-air-ground integrated networks, game theory, and artificial intelligence in 5G networks and beyond. He has published many articles in international journals, such as the *IEEE Journal on Selected Areas in Communications* and the *IEEE Transactions on Vehicular Technology*, as well as articles in conferences, such as the IEEE Wireless Communications and Networking Conference and the IEEE Global Communications Conference.

Baoyun Wang received the PhD degree in electrical engineering from Southeast University, Nanjing, China in 1997. He was a postdoctoral researcher with the Department of Computer Science and Engineering, Pohang University of Science and Technology, Pohang, Republic of Korea from 1999 to 2000, the Department of Electronic Engineering, City University of Hong Kong from 2000 to 2002, and the Department of Mathematics and Computer Science, University of Sydney from 2004 to 2005. He is currently a full professor in electrical engineering with Nanjing University of Posts and Telecommunications, Nanjing. His research interests include the area of statistical signal processing, information theory, and their applications in wireless communications.